



Available online at
<https://jurnalteknik.unisla.ac.id/index.php/CVL>

<https://doi.org/10.30736/col.v2i2>



Static Load Test of the Bridge to Fulfill the Functional Suitability Criteria of Way Sekampung Bridge

Heri Khoeri^{1*}, Panji Nugroho², Wisnu Isvara³

^{1*}Civil Engineering, Faculty of Engineering, Universitas Muhammadiyah Jakarta

²PT. Hesa Laras Cemerlang

³Department of Civil Engineering, Faculty of Engineering, University of Indonesia

Email : ^{1*}heri.khoeri@umj.ac.id, ²kontak@hesa.co.id, ³wisnu.isvara1@ui.ac.id

ARTICLE INFO

Article History :

Article entry : 01-20-2024

Article revised : 02-06-2024

Article received : 03-15-2024

Keywords :

Bridge, Deflection,
Loading, Strain, Static.

IEEE Style in citing this article:

H. Khoeri, P. Nugroho, and W. Isvara, "Static Load Test of the Bridge to Fulfill the Functional Suitability Criteria of Way Sekampung Bridge", *civilla*, vol. 9, no. 1, pp. 11–26, Mar. 2024.

ABSTRACT

Bridges are a crucial transportation infrastructure with a highly significant social function, necessitating the implementation of safety measures for road users as mandated by the Ministry of Public Works and Housing Regulation No. 10 of 2022 on the Security of Bridges and Tunnels. Service ability parameters that must be met for safety include not exceeding stress and deflection limits during operational conditions, including maximum loading. To assess the behavior of the Way Sekampung Bridge during operation, a static load test was conducted. The static load test involved incremental loading up to 64% Uniformly Distributed Load, *UDL* (120 tons) in 16% increments, then followed by a gradual unloading. The measured deflection at 66% *UDL* was 8.698 mm, which extrapolated to 100% *UDL* becomes 17.888 mm, still below the allowable deflection ($L/1000 = 35.7$ mm). Similarly, the strain extrapolated from the 64% *UDL* strain, which is 0.00013, is also below the allowable tensile strain that could potentially cause concrete cracking ($= 0.00015$). Throughout the structural testing stages, the structure exhibited linear elastic behavior, with a residual deflection of 1.3 mm below the allowable residual deflection (17.4 mm). Based on the assessment of static test parameters, the bridge is deemed suitable for operation.

1. Introduction

The Way Sekampung Bridge to be tested is a newly constructed bridge intended to replace the old bridge, as shown in **Figure 1**. It is a 3-span PCI Girder bridge with spans of 35.7 m + 41.2 m + 35.7 m, a traffic width of 7.2 m, and 0.5 m sidewalks on both sides of the bridge. The layout and longitudinal section of the bridge are depicted in **Figure 2**. Before opening to



Copyright © 2024 Heri Khoeri, et al. This work is licensed under a [Creative Commons Attribution-ShareAlike 4.0 International License](https://creativecommons.org/licenses/by-sa/4.0/). Allows readers to read, download, copy, distribute, print, search, or link to the full texts of its articles and allow readers to use them for any other lawful purpose.

general traffic, testing is necessary to ensure the safety of the bridge users. One common assessment method for existing bridges is load testing [1].

The tested span is the first span in the Tanjung Karang direction, consisting of 5 PCI girders with a span of 35.7 m, as illustrated in the cross-section in Figure 3.

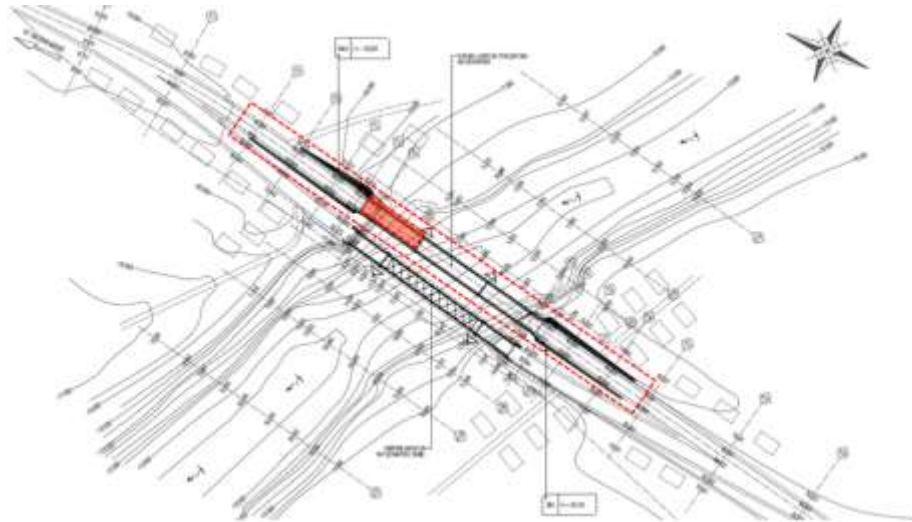


Figure 1. Location and span of the Way Sekampung Bridge to be tested

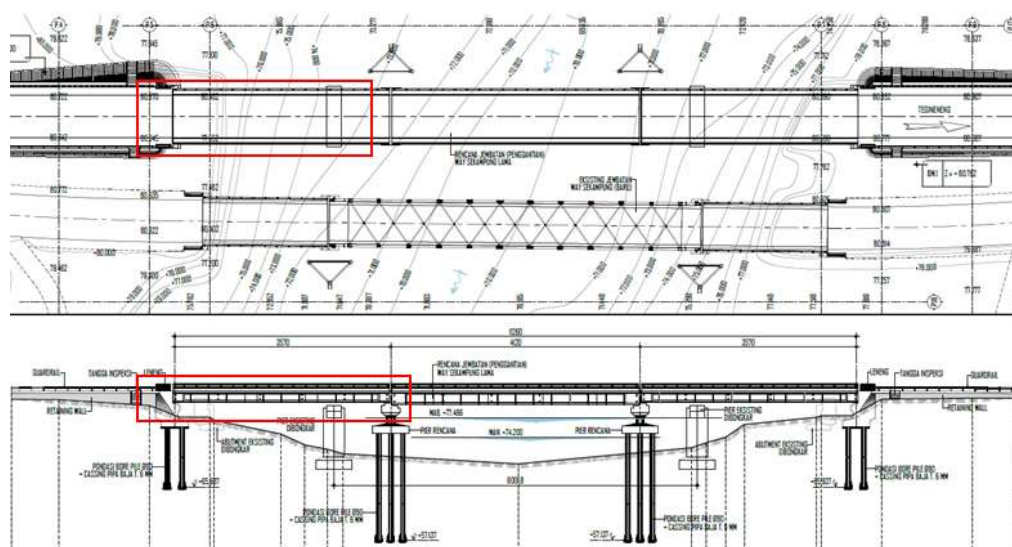


Figure 2. Plan and long section of the Way Sekampung Bridge

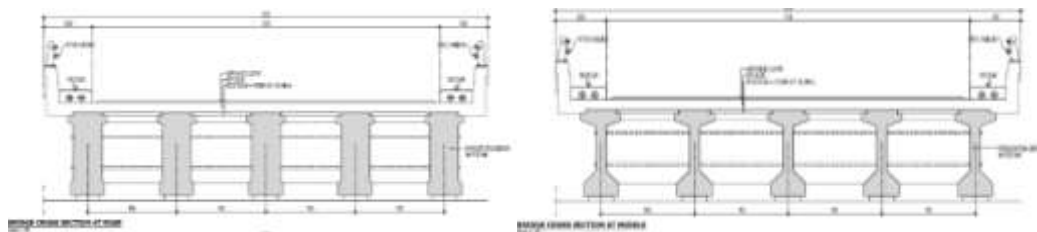


Figure 3. Cross-section of the bridge at the abutment (left) and the mid span (right).

Testing bridges with dynamic load tests is an effective and efficient way to estimate bridge performance under operational conditions. With operational modal analysis (OMA), testing can be conducted without having to close bridge traffic [2]. Alternatively, with experimental modal analysis (EMA), which only requires a relatively short time to close traffic to obtain dynamic response triggers from vehicle impacts, compared to static load tests that

require time for load placement, staging, and response measurements [3]. The test results conducted by PT. Hesa Laras Cemerlang indicate that the bridge is structurally suitable based on dynamic parameters [4]. However, static load testing remains more accurate compared to dynamic load testing because the applied load can be incrementally increased up to the maximum load [5]. And this is feasible because the traffic has not been opened yet.

Static load testing is a common and effective method for assessing the performance of bridges, understanding the actual operational conditions of the bridge, and identifying existing issues promptly to improve and optimize bridge quality [6], [7]. Load testing also serves as a crucial starting point for monitoring operations. There is a strong correlation between the behavior of the bridge during load testing and its long-term behavior [8]. To complement the results of the dynamic load test conducted in the previous study, a static load test was performed to assess the bridge's structural integrity based on parameters such as deflection, strain, and linearity of bridge response.

2. Research Method

The criteria for static load testing used are by the Bridge Testing Implementation Manual, 2012 [8].

2.1 Description and Technical

The test load used is a truck, and the calculation for the test truck configuration is as follows [8]:

- Main span, L (meters)
- Traffic width, b (meters)
- $UDL = 0,9 \times \left(0,5 + \frac{15}{L}\right)$ ton/m²
- $UDL/m' = 5,5UDL + 50\%UDL(b - 5,5)$; Note: If the traffic width, b , is less than 5.5m, then UDL is multiplied by 5.5; if it exceeds, then the remaining traffic width is multiplied by 50% UDL .
- $UDL_{Total} = UDL/m' \times L$
- Following the concept of linearity and assuming the structure is still elastic, 50% of the UDL load will be applied.
- The total UDL_{Total} is divided by the unit weight of the test truck to determine the number of trucks required for static bridge testing.

Following the above provisions, the minimum load to be applied during the bridge test is:

Main span, L	=	35,70 m
Traffic width, b	=	7,20 m
$UDL = 0,9 \times \left(0,5 + \frac{15}{L}\right)$	=	0,83 ton/m ²
$UDL/m' = 5,5UDL + 50\%UDL(b - 5,5)$	=	5,26 ton/m
 $UDL_{Total} = UDL/m' \times L$	 =	 187,74 Ton
Minimum Load (50%)	=	93,87 Ton

The load used during testing:

Truck used	=	8 Truk
Weight of one Truck	=	15 Ton
Total Load	=	120 Ton
	=	64% UDL

Truck specifications are as shown in **Figure 4**.

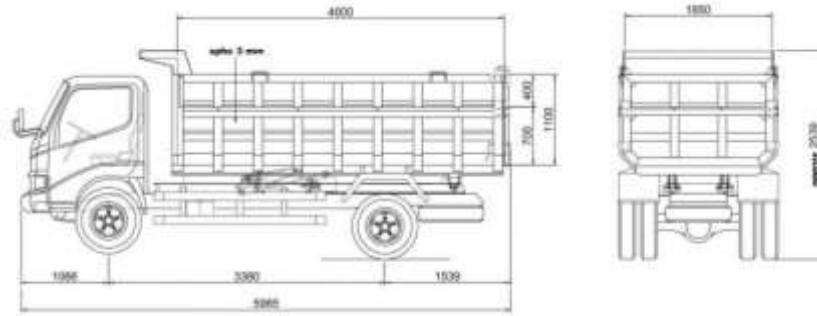
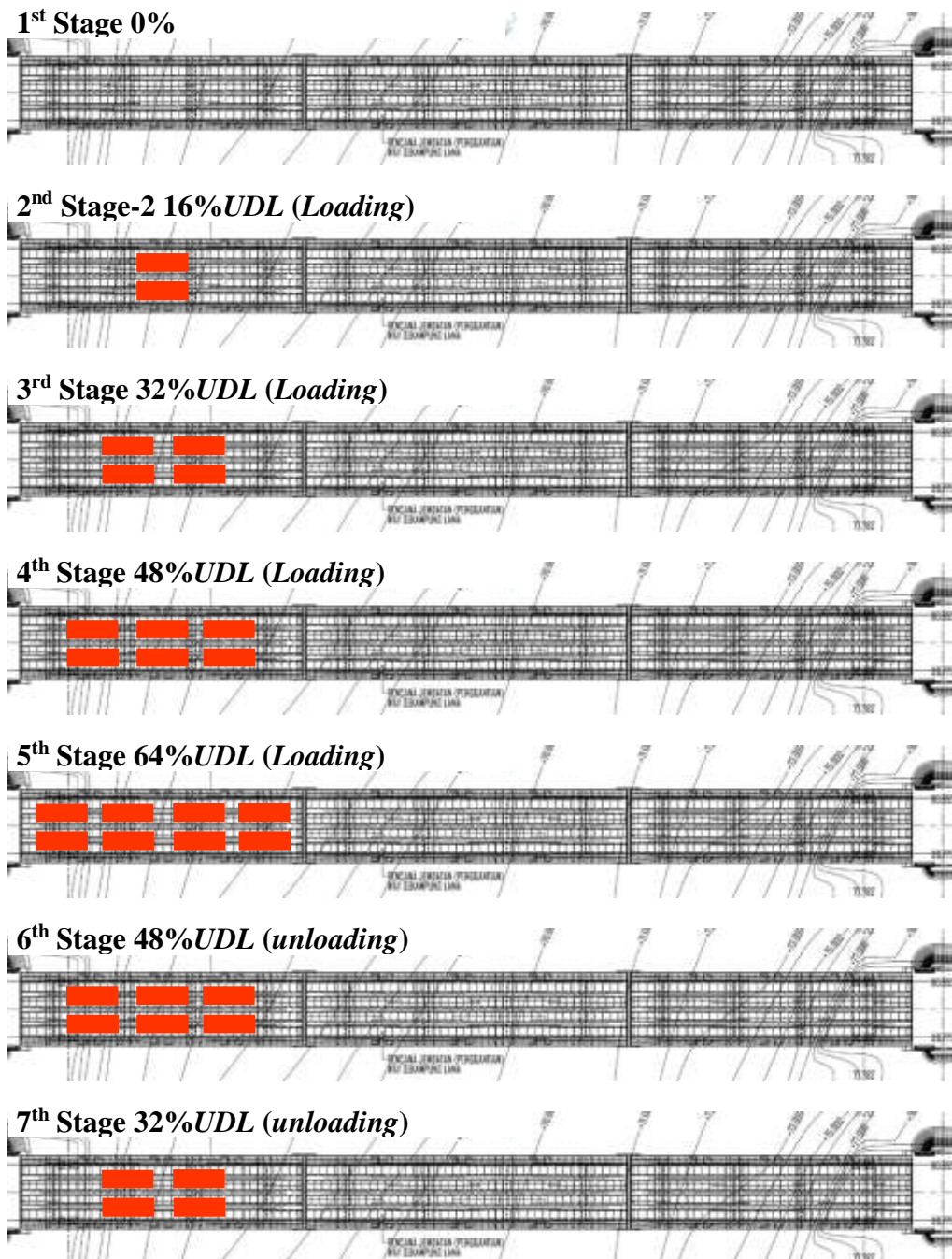


Figure 4. The truck used as a load, with a total weight of 15 tons including the cargo.

Stages and truck loading configurations are as shown in Figure 5 below and Table 1 below:



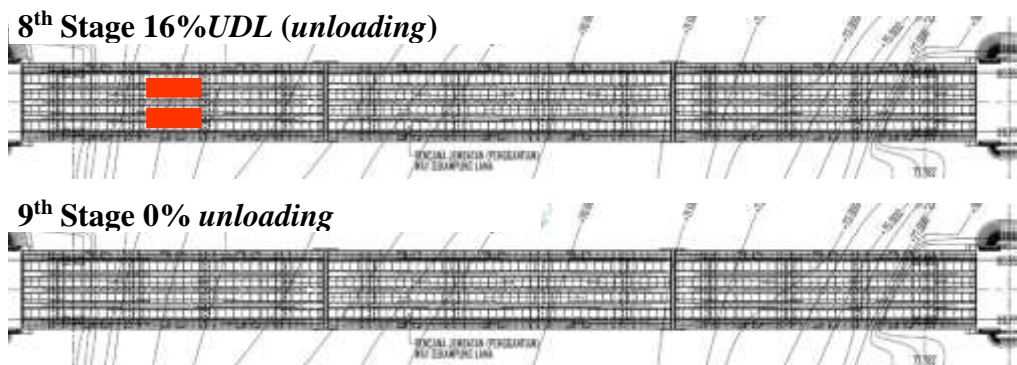


Figure 5. Stages and truck loading configurations

Figure 5 illustrates the loading stage configuration, where the maximum load used in this study is 64%. Considering the span length and truck dimensions to be used as the load, it is divided into 5 stages of load increments: 0%, 16%, 32%, 48%, and 64%. Similarly, in the unloading stage, it is divided into 5 stages: 64%, 48%, 32%, 16%, and 0%. For each increment stage, 2 trucks with a weight of 15 tons each, or 30 tons per load increment, are added. The same incremental approach is applied for unloading stages, as presented in **Table 1**.

Table 1. The stages of loading

The stages of loading	Number of Trucks	Load (Ton)	%UDL
Stage-1	0	0	0%
Stage -2 (Loading)	2	30	16%
Stage -3 (loading)	4	60	32%
Stage -4 (Loading)	6	90	48%
Stage -5 (loading)	8	120	64%
Stage -6 (unloading)	6	90	48%
Stage -7 (unloading)	4	60	32%
Stage -8 (unloading)	2	30	16%
Stage -9 (unloading)	0	0	0%

Source: The calculation results refer to the provisions of Manual 004/BM/2012 [8].

LVDT, Dial Gauge, Strain Gauge, and reflector sheet are placed at $\frac{1}{4}$, $\frac{1}{2}$, and $\frac{3}{4}$ spans and positioned at the bottom of the bridge, as shown in Figure 6.

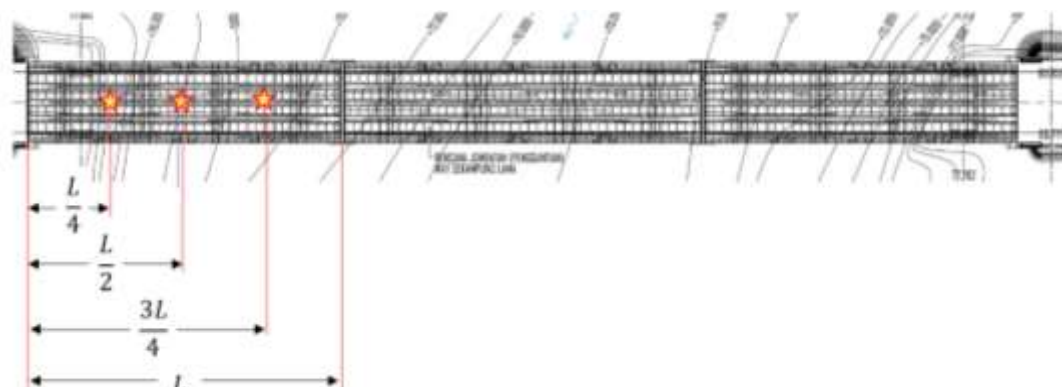

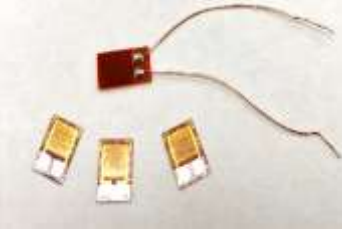






Figure 6. Placement of LVDT, Dial Gauge, Strain Gauge, and reflector sheet

Sensors and measuring instruments used for static load testing are as listed in **Table 2**.

Table 2. Sensors and measuring instruments used for static load testing

No	Description	Technical Data
1	LVDT (Linear Variable Differential Transformer) GT2 - H50 	<ul style="list-style-type: none"> ▪ Detection System = Scale Shot System, Absolute (No Tracking Errors) Type ▪ Measuring Range = 50 mm; Resolution (20oC) = 0.5 μm; Indicate Accuracy = 3.5 μm (P-P) ▪ Measuring Force: Downward Mounting = 3.2 N; Side Mounting = 2.8 N; Upward Mounting = 2.4 N ▪ Sampling Cycle = 1 ms; Mechanical Response = 7 Hz ▪ Operation Indicator = 2 - Colour LED (Red, Green) ▪ Environmental Resistance: Enclosure Rating = IP67 (IEC); Ambient Temperatue = -10 to 55 oC (No Freezing); Relative Humidity = 35 to 85 % RH (No Condensation); Vibration = 10 to 55 Hz Double Amplitude 1.5 mm in The X, Y, Z Axis Directions Respectively, 2 Hours
2	Rosette Strain Gauge 3 Axis Hesa GT2 - H50 	<ul style="list-style-type: none"> ▪ Gage Factor 120 (23oC, 50%) = 2.04 1.0% ▪ Gage Length = 1 mm ▪ Gage Resistance (23oC, 50%) = 120.4 Ohm 0.4% ▪ Transverse Sensitivity Ratio = ▪ Thermal Output = Refer to Graph ▪ Temperature Compensation for = Steel ▪ Adoptable Thermal Expansion = $11.7 \times 10^{-6} / \text{oC}$ ▪ Aplicable Adhesive = CC-33A, EP-340 ▪ Temperature Coefficient of Gage Factor = Refer to Graph
3	Data Logger & Acquistion Hesa RS485 	<ul style="list-style-type: none"> ▪ Clock speed = 16 MHz ▪ Memory = up to 64 gb ▪ Data communication = NRF2410 N 2,4 Ghz, Rs485, USB 3.0 ▪ UP to 12 Channel
4	Dial Gauge 3052S-19 MITUTOYO 	<ul style="list-style-type: none"> ▪ Measuring force: 2.5 N or less ▪ Maximum Measurement : 0-30 mm ▪ Additional Features : Shockproof, Jeweled Bearing, Revolution Counter ▪ Display : 0-100 ▪ Item Weight : 0.62 pounds ▪ Measurement Accuracy : +/-0.025 mm ▪ Outside Diameter : 78 mm ▪ Range : 0-30 mm ▪ Resolution : 0.01 mm
5	Total Station Nikon Nivo 5C	<ul style="list-style-type: none"> ▪ Tilt Accuration : 5'' ▪ Display : <ul style="list-style-type: none"> ○ F1 – QVGA, 16Bit Colour, TFT LCD, Backlit (320x240 pixel) with QWERTY touch-screen alpha-numeric and transcriber keypad ○ F2 – Backlit Graphic LCD (128x64 pixel) ▪ Compensator : Dual Axis <ul style="list-style-type: none"> ○ EDM Type : Reflectorless ○ Distance Acuracy: 3 mm + 2 ppm

No	Description	Technical Data
		○ Range distance : 5,000 m Single Prism / 300 m Prismless
6	Reflector Sheet 	<ul style="list-style-type: none"> ▪ Dimension 5 cm x 5 cm ▪ Material = Fiber glass

Source: The researcher's interpretation results to fulfill the test data requirements according to MANUAL 004/BM/2012 [8].

The LVDT data, dial gauge data, and TS (strain gauge) data are all used to measure deflection, and their characteristics crosscheck each other. The LVDT has precision up to 10^{-6} m, Dial gauge 10^{-5} m, and TS 10^{-3} m. Since the loading stages are linear, and the measurement points are theoretically positioned, anomalies in the data will be approximated with measurement values close to theoretical values. However, if the LVDT data, dial gauge data, and TS data are close in value, the LVDT data will be used due to its precision up to μm .

The displacement of the structure due to static loading can be measured in both horizontal and vertical directions. However, vertical displacement, commonly expressed as structural deformation, is typically measured in each case using dial gauges (strain gauges), fabricated LVDTs, flatness measurements, or other measurement techniques [8]

The measured values of displacement, mostly deformation, are compared with calculated values corresponding to standard loads, design loads, and loads applied during testing. Measured values are usually smaller than calculated values because even highly complex calculation models (even when using computers) are always simpler than real structures. When the opposite situation occurs, it indicates that the structural damage process has reached an advanced stage. However, when the transverse interaction of structural elements is tested under non-uniform loading, calculated values may be less than measured values in some parts of the structure. This indicates that the real transverse interaction is better than the one produced by the calculation model [[8], [9], [10], [11], and others]. The maximum allowable deflection refers to Table 3 below:

Table 3. Maximum allowable deflection [12], [13]

Element Type	Reviewed Deflection	Allowable deflection	
		Vehicle Load	Vehicle & Pedestrian Load
Simple beam or continuous	Instantaneous deflection due to live load and impact load	L/800	L/1000
Cantilever		L/400	L/375

One fundamental measure of structural quality is the elastic behavior of the bridge under loading and unloading cycles. The maximum allowable permanent deflection (Δ_p) after the removal of the load is generally specified in relevant regulations or standards as a fraction

of the maximum deflection (Δ_{max}) under loading [8]. In this test, the limit for permanent deflection is set at [14]:

$$\Delta_p < 0.2\Delta_{max} \quad (1)$$

The stress-strain curve for concrete is roughly linearly elastic until the maximum tensile strength is reached. Beyond this point, concrete cracks, and the strength gradually decreases to zero [[15], [16], [17], [18]]. Figure 7 illustrates the typical stress-strain relationship in concrete.

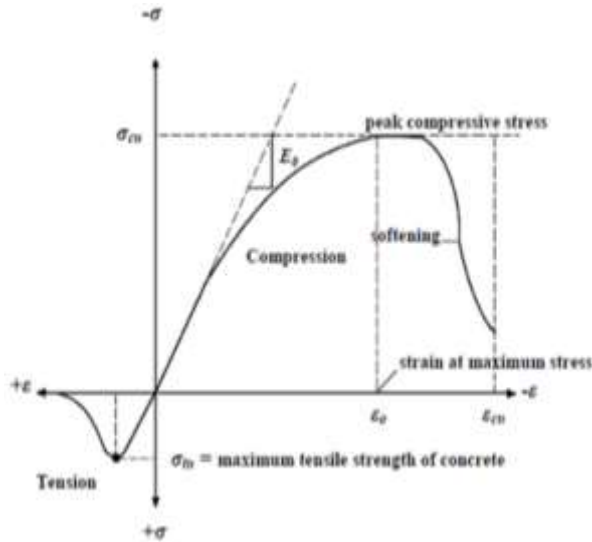


Figure 7. Typical stress-strain relationship in concrete [18]

Referring to the Wika Beton brochure [19], girders for a span of 35.7m use concrete with $f_c' = 50$ MPa. Therefore, the stress-strain relationship for concrete from Mander for $f_c' = 50$ MPa is as shown in **Figure 8**.

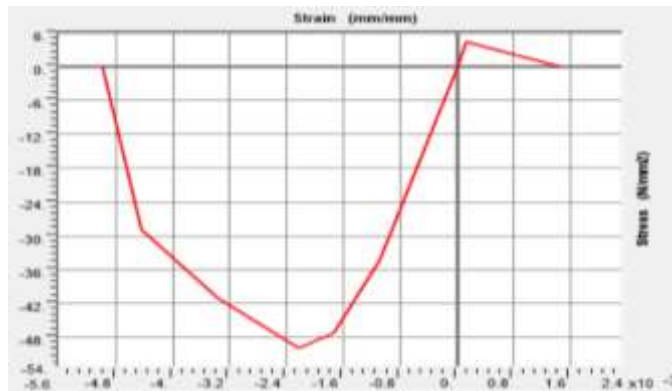


Figure 8. Stress-strain relationship of concrete $f_c' = 50$ MPa

Refer to **Figure 8**, Allowable strain (elastic) on girder $f_c' = 50$ MPa:

$$\begin{aligned} \epsilon_{max} &= 0,000133 \rightarrow \sigma = 4,4 \text{ MPa (tension)} \\ \epsilon_{min} &= -0.001083 \rightarrow \sigma = -34.24 \text{ MPa (compression)} \end{aligned} \quad (2)$$

4. Results and Discussions

All initial values at the stage before loading are considered as benchmarks (if not valued at 0, the measured values will be subtracted from the values of the subsequent stage).



Figure 9. Documentation of the 16% UDL loading

Table 4. Data on static deflection at 16% UDL

Load (UDL)	Sensor/ Measuring Instrument	Deflection (mm)				
		0	L/4	L/2	3L/4	L
16% (30 ton)	LVDT	0	1.839	2.826	1.554	0
	Dial	0	2.32	2.97	1.97	0
	TS	0	2	3	2	0
	Allowable	0	3.998	5.712	3.998	0

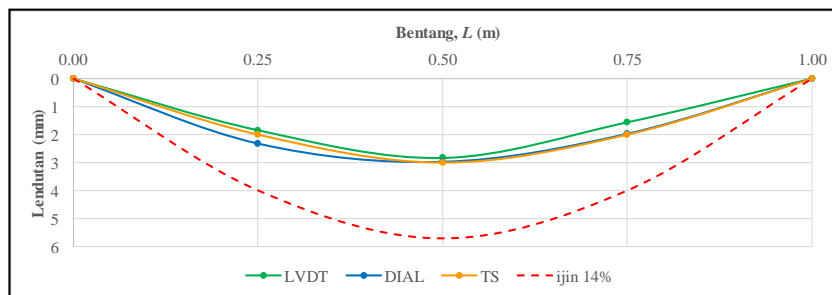


Figure 10. Static deflection of 16% UDL loading

The maximum deflection that occurred is less than the allowable deflection projection; thus, the test proceeds to a 32% loading, with loading documentation as shown in **Figure 11**.



Figure 11. Documentation of the 32% UDL loading

Table 5. Data on static deflection at 32% UDL

Load (UDL)	Sensor/ Measuring Instrument	Deflection (mm)				
		0	L/4	L/2	0	L
32% (60 ton)	LVDT	0	3.361	5.000	3.076	0
	Dial	0	3.54	5.26	2.83	0
	TS	0	4	6	3	0
	Allowable	0	7.997	11.424	7.997	0

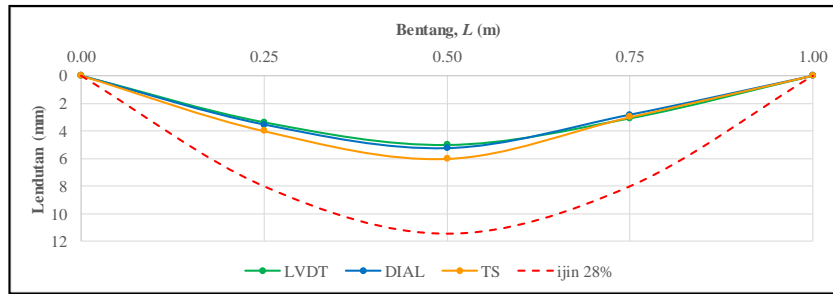


Figure 12. Static deflection of 32% UDL loading

The maximum deflection that occurred is less than the allowable deflection projection; thus, the test proceeds to a 48% loading, with loading documentation as shown in **Figure 13**.



Figure 13. Documentation of the 48% UDL loading

Table 6. Data on static deflection at 48% UDL

Load (UDL)	Sensor/ Measuring Instrument	Deflection (mm)				
		0	L/4	L/2	0	L
48% (90 ton)	LVDT	0	4.883	6.957	4.380	0
	Dial	0	5.00	7.22	5.26	0
	TS	0	5	7	4	0
	Allowable	0	11.995	17.136	11.995	0

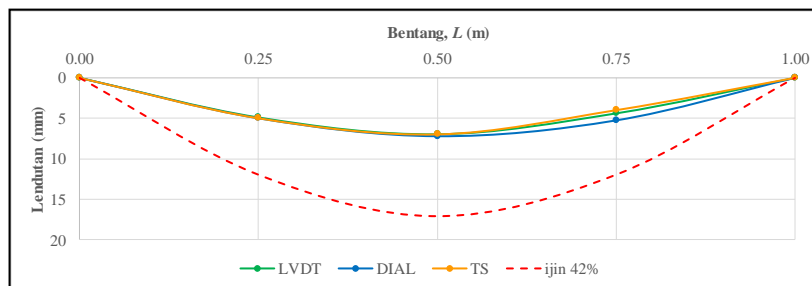


Figure 14. Static deflection of 48% UDL loading

The maximum deflection that occurred is less than the allowable deflection projection; thus, the test proceeds to a 64% loading, with loading documentation as shown in **Figure 15**.



Figure 15. Documentation of the 64% UDL loading

Table 7. Data on static deflection at 64% UDL

Load (UDL)	Sensor/ Measuring Instrument	Deflection (mm)				
		0	L/4	L/2	0	L
64% (120 ton)	LVDT	0	5.274	8.696	5.185	0
	Dial	0	6.22	9.51	6.12	0
	TS	0	7	9	6	0
	Allowable	0	15.994	22.848	15.994	0

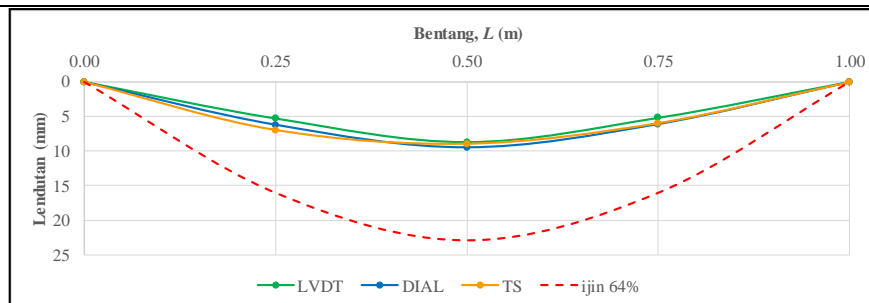


Figure 16. Static deflection of 64% UDL loading

Table 8. Data of static deflection during the unloading stage from 64% to 0% UDL

Load (UDL)	Sensor/ Measuring Instrument	Deflection (mm)				
		0	L/4	L/2	0	L
Unloading from 64% to 48%	LVDT	0	4.943	7.087	4.404	0
	Dial	0	5.10	7.42	5.41	0
	TS	0	5	8	5	0
Unloading from 48% to 32%	LVDT	0	3.413	5.130	2.978	0
	Dial	0	3.71	5.50	3.02	0
	TS	0	4	5	4	0
Unloading from 32% to 16%	LVDT	0	1.848	2.957	1.413	0
	Dial	0	2.00	3.23	2.30	0
	TS	0	3	4	3	0
Unloading from 16% to 0% (permanent load)	LVDT	0	0.041	0.130	0.016	0
	Dial	0	0.1	0.2	0.15	0
	TS	0	1	1	1	0
permanent load	Allowable	0	1.055	1,391	1.055	0

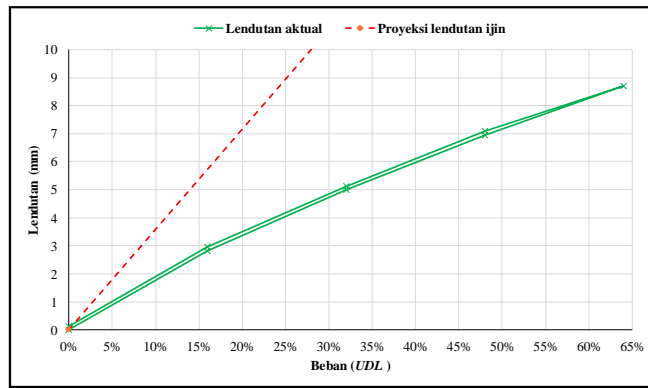


Figure 17. Deflection due to *loading-unloading UDL*

Table 9. Data of static strain at the mid-span

UDL	ϵ
0%	0
16%	0.00001375
32%	0.00003361
48%	0.00005348
64%	0.00007470
48%	0.00005562
32%	0.00003462
16%	0.00001485
0%	0.00000186

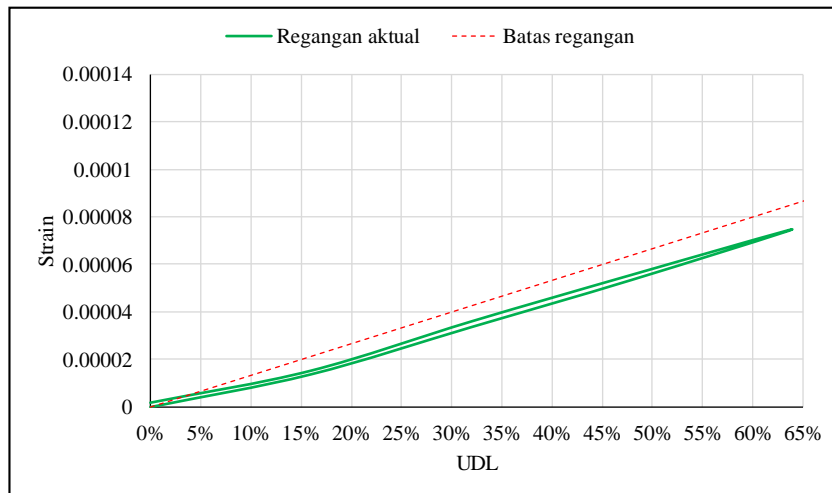


Figure 18. Strain due to *loading-unloading UDL*

Based on the graphs in **Figure 10**, **Figure 12**, **Figure 14**, and **Figure 16**, created from the data in **Table 4**, **Table 5**, **Table 6**, and **Table 7**, it is evident that the deflection observed remains below the allowed maximum deflection projection.

Considering that the deflection patterns between LVDT, Dial gauge, and TS are almost identical, further discussion will use LVDT data, as it has the highest level of precision (μm). Based on the graph illustrating the linear relationship between the addition and reduction of loads against deflection (**Figure 17**), indicates that the structure remains elastic during loading. The residual (permanent) deflection is only 0.13 mm, which is significantly less than the allowed permanent deflection ($=1.391$ mm).

Considering that the observed deflection is only 38.1% of the theoretical deflection and the linear relationship between the increase in load and the increase in deflection, the deflection at 100% UDL can be projected, as shown in **Figure 19**.

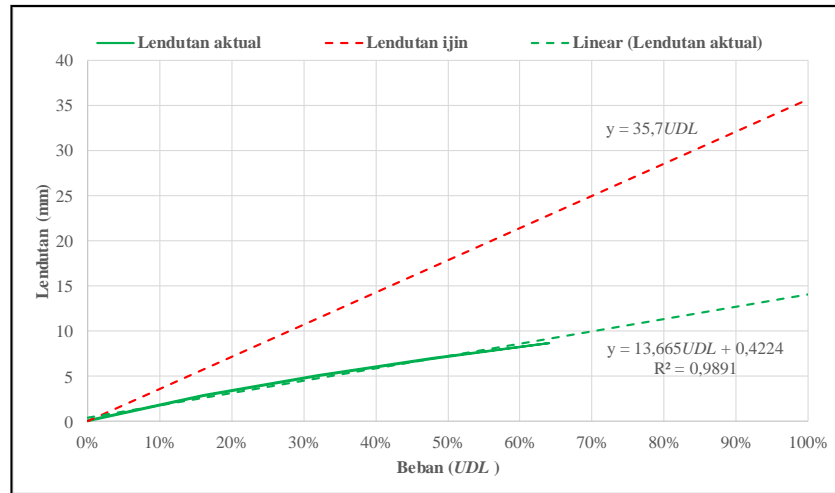


Figure 19. Projection of deflection at 100% UDL

In line with the deflection, the strain measurement results also show the same outcome. The measured strain at each stage of load addition and reduction indicates that the bridge structure is in a linear elastic condition. The strain that occurs during the loading process does not lead to tensile strain causing cracking. This result is demonstrated by plotting the strain values from **Table 9** into the graph in **Figure 8**, with the results shown in **Figure 18**.

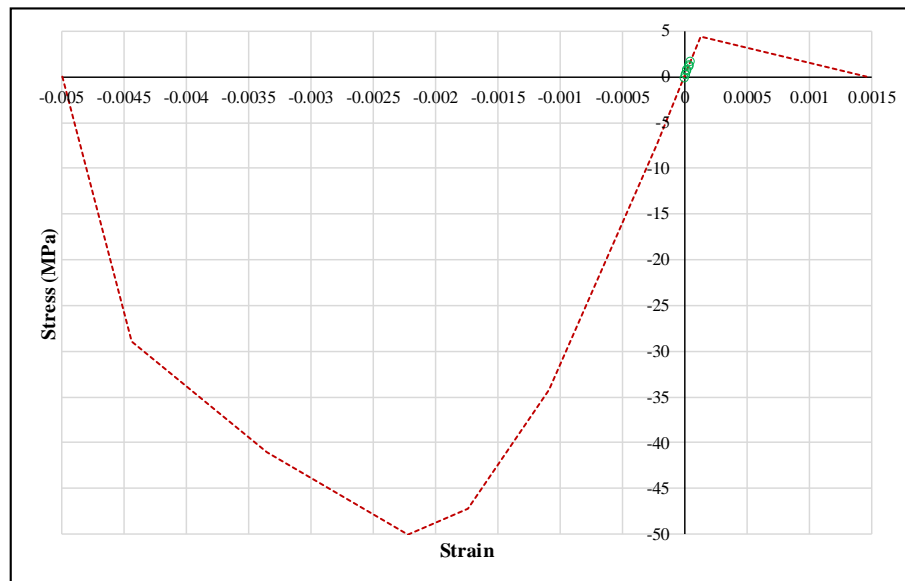


Figure 20. Stress-strain relationship for $f_c' = 50$ MPa

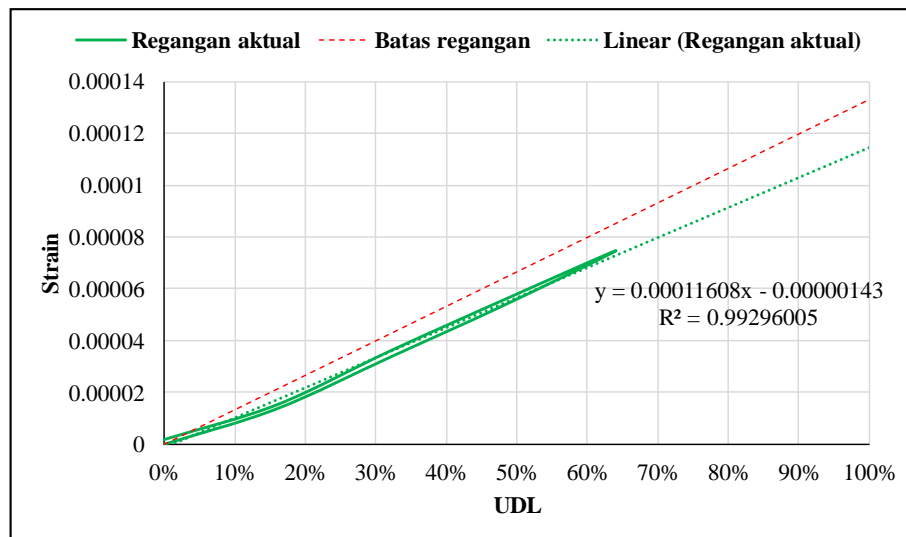


Figure 21. Projection of strain at 100% UDL

If projected to 100% UDL, the strain that occurs, $\varepsilon = 0,0001 \times UDL - 10^{-6} = 0,000116068 \times 100\% - 1,43 \times 10^{-6} = 0,00011465$, and the tensile stress that occurs, $\sigma = 32502 \times \varepsilon - 0.1668 = 32502 \times 0,000115 - 0.1668 = 3,56 \text{ MPa} < 4,4 \text{ MPa}$. Under these conditions, it is estimated that during 100% UDL loading, the concrete in a linear elastic condition will not result in cracking.

5. Conclusion and Suggestion

5.1 Conclusion

The results of the static test indicate that during the loading stages (0%, 16%, 32%, 48%, 64% UDL) and unloading stages (48%, 32%, 16%, 0%), the bridge structure remains linearly elastic. The observed deflections are still below the allowed limits, with an indication that at 64% load, the deflection is 8.696 mm, much less than 64% allowable deflection (64% $L/1000 = 22.848 \text{ mm}$). From the linearity of the test results, the deflection at 100% UDL can be estimated at 17.882 mm, which is 50.11% of the allowable deflection. Thus, it is concluded that the Way Sekampung Bridge meets the criteria for functional suitability based on static load testing.

5.1 Suggestion

For further research, a comparison can be made between the bridge capacity based on the results of static load testing and the results of dynamic load testing, which can serve as input for accurately assessing the bridge's performance using dynamic testing approaches, either with EMA or OMA.

References

- [1] E. O. L. Lantsoght, "Assessment of existing concrete bridges by load testing: barriers to code implementation and proposed solutions," *Structure and Infrastructure Engineering*, pp. 1–13, Oct. 2023, doi: 10.1080/15732479.2023.2264825.
- [2] H. Khoeri, S. W. Alisjahbana, and P. Nugroho, "Uji Beban Dinamik dan Analisis Modal Operasional Jembatan Baja Komposit Underpass Bekambit," *Dinamika Rekayasa*, vol. 20, no. 1, pp. 65–75, Jan. 2024, doi: 10.20884/1.dinarek.2024.20.1.20.
- [3] H. Khoeri, W. Isvara, D. Sofiana, and F. Natasa, "Penilaian Kelaikan Jembatan Berdasarkan Parameter Dinamis Experimental pada Jembatan PC-I Girder 40 m," *Jurnal Aplikasi Teknik Sipil*, 2024.

- [4] PT. Hesa Laras Cemerlang, “Laporan Uji Beban Dinamik Jembatan Way Sekampung,” Dec. 2023. [Online]. Available: <https://hesa.co.id>
- [5] H. Khoeri, S. W. Alisjahbana, J. Widjajakusuma, and N. Najid, “Estimasi Lendutan Pelat Untuk Menghitung Kapasitas Beban Dengan Akurasi Tinggi Menggunakan Uji Getar,” *Konstruksia*, vol. 14, no. 2, pp. 175–188, Jul. 2023, doi: 10.24853/jk.14.2.175-188.
- [6] K. Tu, Y. Ye, D. Wu, Y. Zhou, and W. Deng, “Technical Analysis of Highway Bridge Static Load Test,” *Journal of Architectural Research and Development*, vol. 7, no. 3, pp. 58–63, May 2023, doi: 10.26689/jard.v7i3.4829.
- [7] B. Li, H. Liu, J. Jian, and H. Gao, “Static Load Test Analysis of T-Beam Bridge Shear Strengthening by Prestressed Steel Wire Rope Embedded in Polyurethane Cement (PSWR-PUC),” *Sustainability*, vol. 15, no. 13, p. 10514, Jul. 2023, doi: 10.3390/su151310514.
- [8] Direktorat Jenderal Bina Marga Departemen Pekerjaan Umum Republik Indonesia, *Manual Pelaksanaan Pengujian Jembatan*. 2012.
- [9] PT. Hesa Laras Cemerlang, “Laporan Uji beban Statik dan Dinamik Fly Over Tarahan, Lampung,” 2019. Accessed: Dec. 22, 2023. [Online]. Available: <https://hesa.co.id>
- [10] PT. Hesa Laras Cemerlang, “Laporan Uji Statik dan Dinamik 4 (Empat) Jembatan PT. Hindoli-Cargill di Provinsi Jambi,” 2021. Accessed: Dec. 22, 2023. [Online]. Available: <https://hesa.co.id>
- [11] PT. Hesa Laras Cemerlang, “Laporan Akhir Pengujian Jembatan Tri Martani PT. Borneo Indobara di Kalimantan Selatan,” 2019. Accessed: Dec. 22, 2023. [Online]. Available: <https://hesa.co.id>
- [12] Badan Standardisasi Nasional, *SNI 1725: 2016, Pembebanan untuk Jembatan*. 2016.
- [13] Directorate General of Highways Ministry of Public Works Republic of Indonesia, *Bridge Design Manual, Vol-1*. 1992.
- [14] Badan Standardisasi Nasional, *SNI 2847: 2019; Persyaratan Beton Struktural untuk Bangunan Gedung*. 2019.
- [15] J. F. Georgin and J. M. Reynouard, “Modeling of structures subjected to impact: concrete behaviour under high strain rate,” *Cem Concr Compos*, vol. 25, no. 1, pp. 131–143, Jan. 2003, doi: 10.1016/S0958-9465(01)00060-9.
- [16] D. M. Cotsovos and M. N. Pavlović, “Numerical investigation of concrete subjected to high rates of uniaxial tensile loading,” *Int J Impact Eng*, vol. 35, no. 5, pp. 319–335, May 2008, doi: 10.1016/j.ijimpeng.2007.03.006.
- [17] M. R. Zhou, “Application of Finite Element Method for Nonlinear Analysis in Reinforced Concrete Structures,” *Applied Mechanics and Materials*, vol. 166–169, pp. 935–938, May 2012, doi: 10.4028/www.scientific.net/AMM.166-169.935.
- [18] M. Y. H. Bangash, *Concrete and concrete structures: numerical modelling and applications*. London: Elsevier Applied Science, 1989.
- [19] Wika Beton, “The Precast Concrete Manufacture,” Apr. 2019 Accessed: Dec. 05, 2023. [Online]. Available: <https://wika-beton.co.id/uploads/1-BROSURSET.pdf>

This page is intentionally left blank